EXPERIMENTAL MEASUREMENTS OF THE SPACE SHUTTLE MAIN ENGINE FUEL AND OXYGEN TURBOPUMP VIBRATION CHARACTERISTICS

Edgar J. Gunter
Professor
Director, Rotor Dynamics Laboratory
Dept. of Mechanical & Aerospace Engineering
University of Virginia
Charlottesville, Virginia

Ronald D. Flack
Assistant Professor
Dept. of Mechanical & Aerospace Engineering
University of Virginia
Charlottesville, Virginia

ABSTRACT

The vibration characteristics of the SSME (space shuttle main engine) are dealt with. The space shuttle engine consists of a main rocket nozzle and attached to it are high pressure fuel and oxygen pumps. Various vibration problems have been encountered with both the hydrogen and oxygen pumps. The vibration spectrum of the hydrogen and oxygen pumps has been analyzed by various techniques using synchronous tracking filters and FFT analyzers. The experimental data has been correlated to theoretical predictions of resonance frequencies.

INTRODUCTION

For the past four years, the Rotor Dynamics Laboratory of the University of Virginia has investigated various aspects of the dynamic and stability characteristics of the space shuttle main engine (SSME) high pressure hydrogen and oxygen pumps. A schematic of the SSME is shown in Figure 1. The purpose of this paper is to present some of the experimental techniques used in the investigation of the vibration phenomena encountered with the hydrogen and oxygen pumps.

HYDROGEN TURBOPUMP THEORETICAL ANALYSIS

The SSME engine has two high speed rotating pumps, one for liquid hydrogen and one for liquid oxygen. The schematic diagram of the hydrogen pump is shown in Figure 2. The hydrogen pump is designed to operate at 37,500 RPM. It has two turbine stages which drive three radial pump impellers. Although the hydrogen pump only weighs approximately 125 lbs, the two stages of turbine are designed to develop up to 72,000 horsepower. This pump therefore is one of the highest energy density pumps ever developed. In the original testing of the hydrogen pump, a self-excited instability was observed at approximately 20,000 RPM. The operating pump speed could not exceed this value for a prolonged length of the time without causing bearing or pump damage. The occurrence of the stability problem was predicted by Childs (1). A stability analysis of the hydrogen pump was conducted by the Rotor Dynamics Laboratory. In the original design of the hydrogen pump, the rotor was supported by soft bearing mounts in order to lower the rotor critical speed below the operating speed range. The seals alone acting on the rotor were sufficient to cause self-excited whirl stability. The Rotor Dynamics group at the University of Virginia predicted that a dramatic increase in the stability threshold speed of the hydrogen pump could be obtained by stiffening the bearing supports and replacing the labyrinth seals with smooth, straight seals (2,3). These changes were incorporated into the pump and the stability problem has been eliminated (4).

However, in the process of eliminating the stability problem, the stiffened bearing supports and seals raise the critical speeds. Early data analysis of the hydrogen pump indicated that the bearing support stiffnesses are lower than the originally anticipated design values. This places the hydrogen pump second critical speed in the operating speed range. However, when a spectrum analysis was made of some of the earlier runs, various resonance frequencies were observed which were not predicted by original critical speed analysis.

A more complex dynamic analysis was considered to include the flexible pump casing and the hot gas manifold which attaches to the main engine. This more elaborate analysis gave rise to the prediction of combined axial, radial, and lateral rotor-casing modes. For example, Figure 3 represents the predicted hydrogen pump critical speeds corresponding to the in-plane direction. Depending upon the assumed values of the balance piston and the bearing stiffnesses, it is possible to have several hydrogen pump critical speeds in the operating speed range (5).

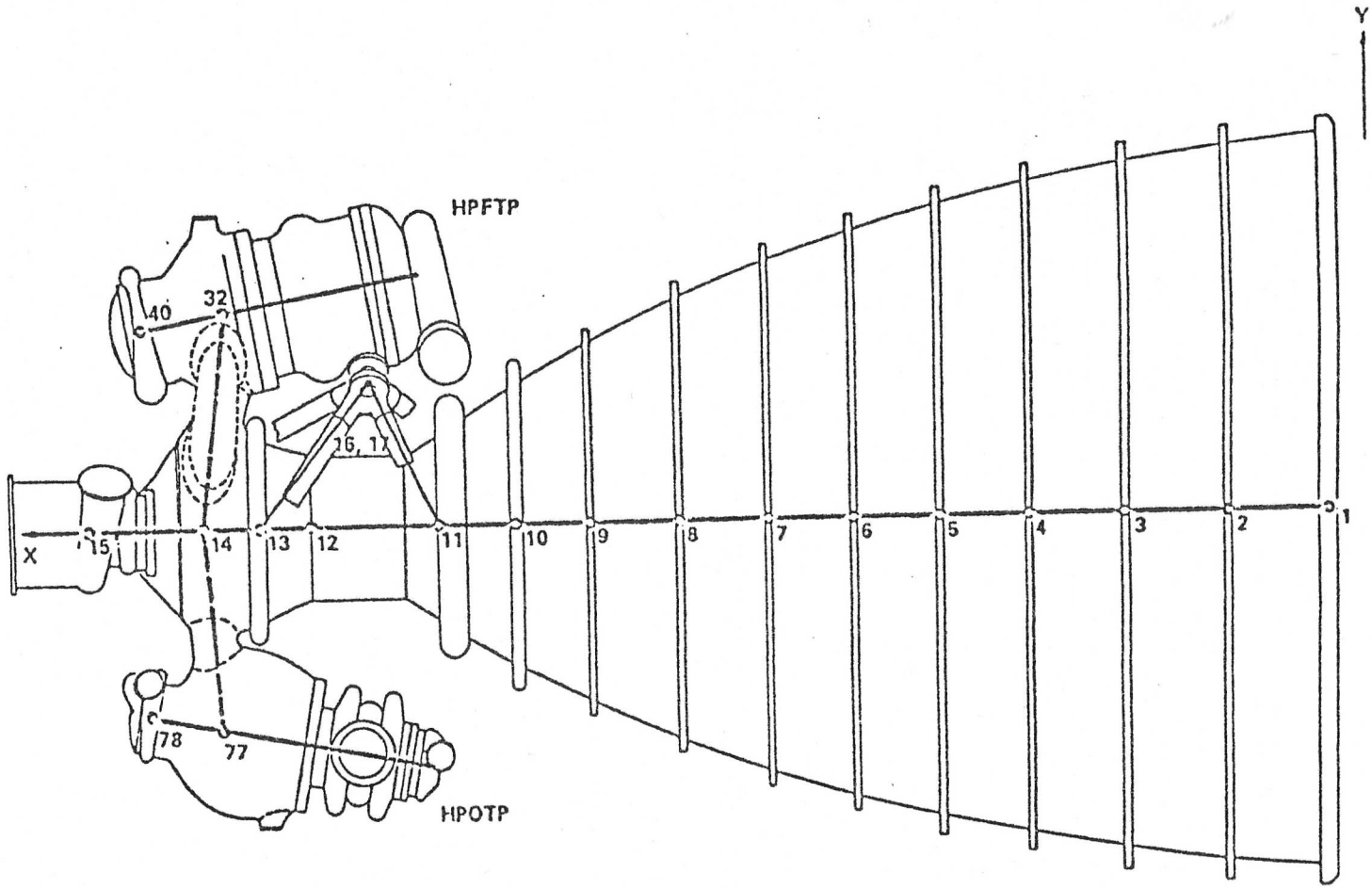

FIG 1 SPACE SHUTTLE MAIN ENGINE(SSME)

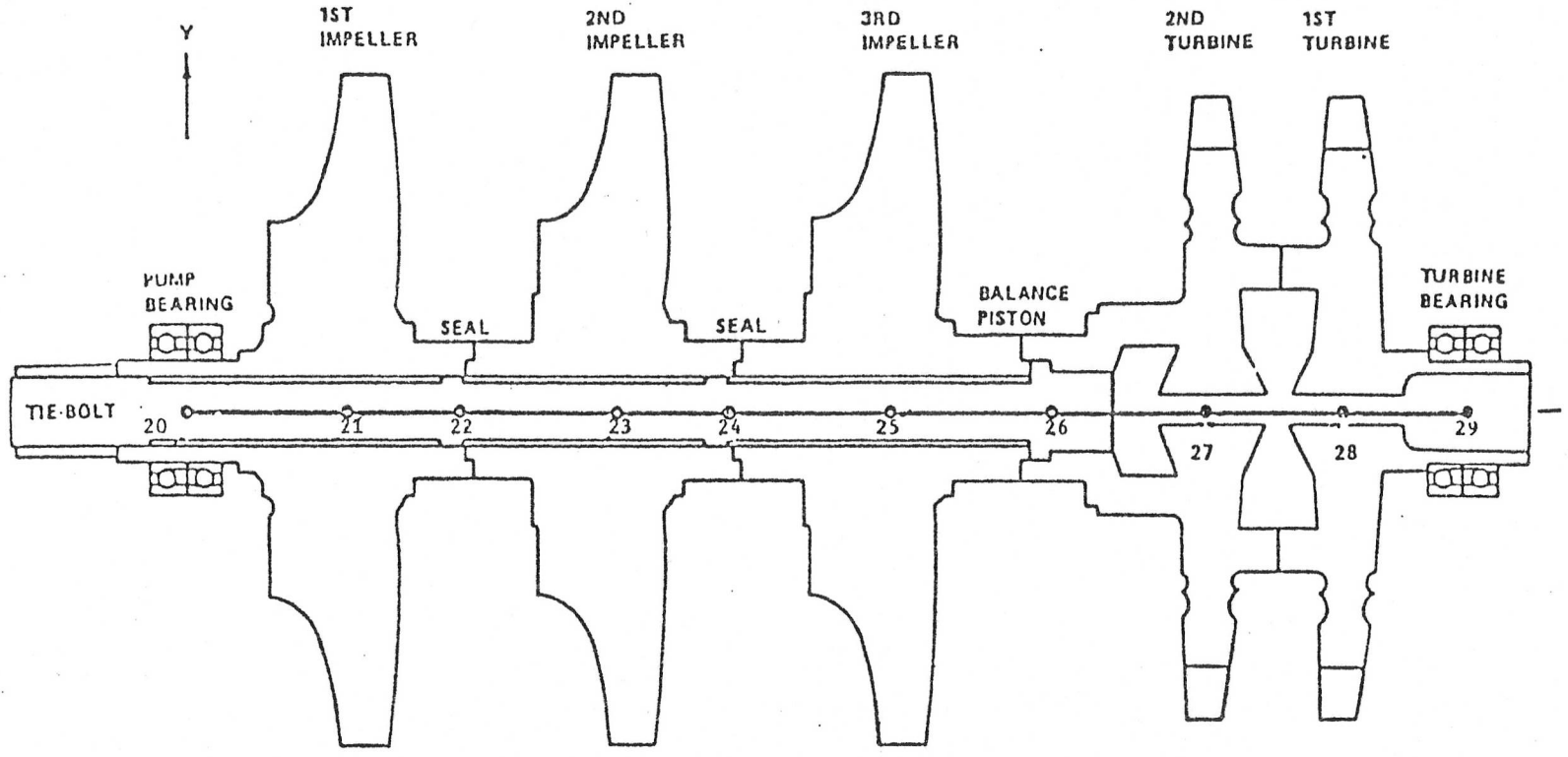

FIG 2 HYDROGEN PUMP CROSS SECTION

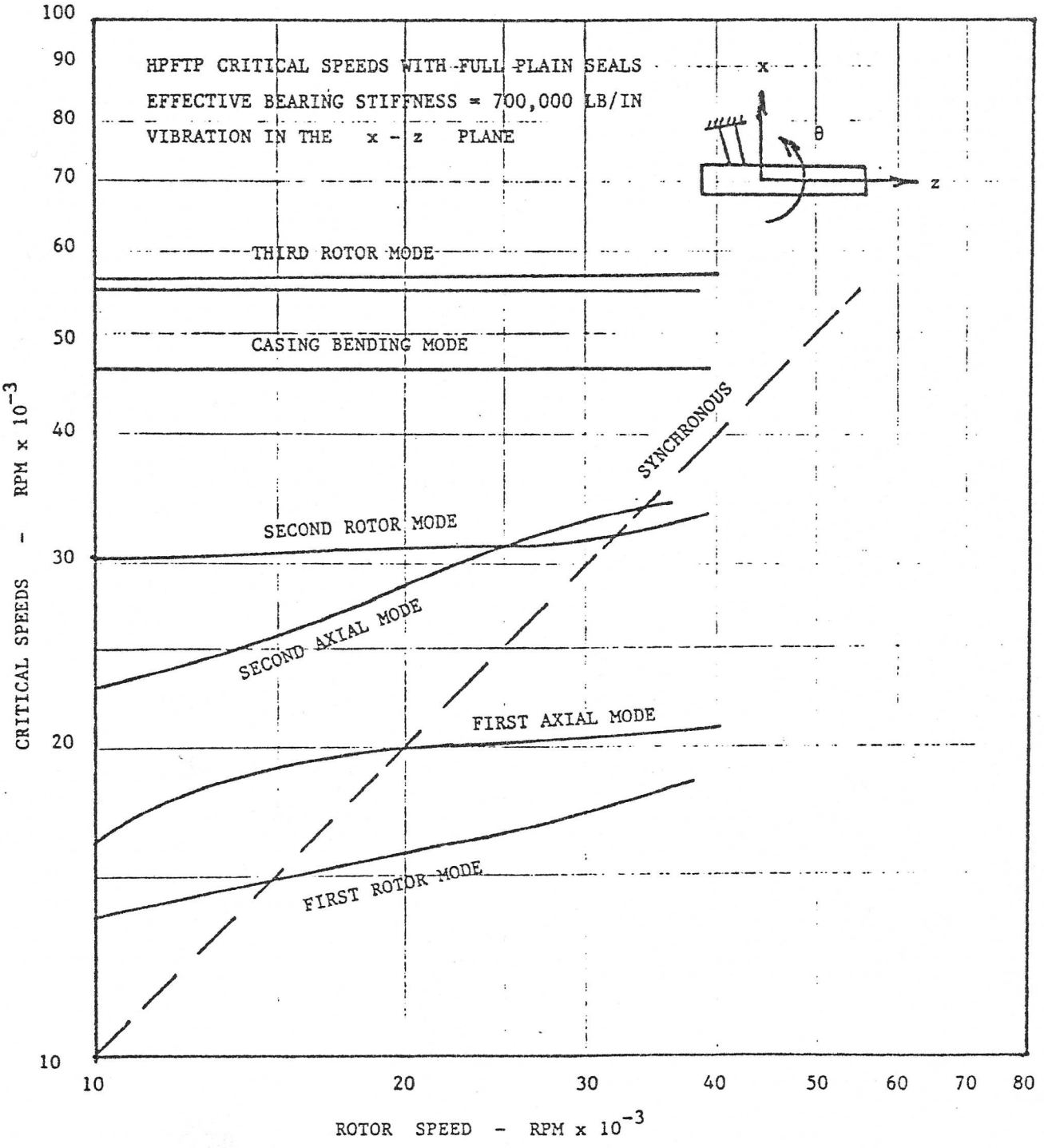

FIG 3 HYDROGEN PUMP CRITICAL SPEED PLOT

HYDROGEN PUMP EXPERIMENTAL INVESTIGATION

The instrumentation available on the hydrogen pump consists of various accelerometers located on the pump casing and internal proximity probes to monitor the relative shaft motion. In order to determine the presence of a rotor critical speed, it is necessary to perform synchronous tracking on either the output of the proximity probe monitoring the shaft motion, or the output of the accelerometers on the casing. To perform synchronous tracking, one must have a reference timing signal generated by shaft rotation. The reference timing signal and the particular vibration signal to be monitored are then input into a synchronous tracking filter to determine amplitude and phase.

Two tracking filters were used in this phase of the study; the Spectral Dynamics SD 119 Trim Balance Analyzer, and the Bently Digital Vector Filter 2. The Bently tracking filter may be used to record total, synchronous, or nonsynchronous motion as a function of shaft speed.

Unfortunately, the turbopump speed control signal is a four pulse-per-shaft-revolution signal, instead of a single pulse. Elaborate procedures had to be developed in order to produce a single pulse for the tracking filters. Figure 4 represents a schematic of the instrumentation employed to produce a single timing signal for triggering the Bently Nevada tracking filter.

Generally, three data analysis procedures are used: (1) plotting of the total vibration amplitudes against turbopump shaft speed, (2) plotting of the synchronous component of the vibration and phase versus shaft speed, and (3) frequency spectrum analysis of the vibration signal. Of these three methods, the latter two are the most useful. The presence of a great deal of noise on the total vibration signal makes the first type of plots practically useless. The vibration data was recorded on one inch tape at 64"/sec and was played back on a 14 channel FM tape recorder at reduced speed. The record times were monitored by means of a time code reader. The channel with speed pick-up four pulses per revolution was first conditioned with a smoothing filter. It was then fed into a Spectral Dynamics Tracking Ratio Tuner, Model SD 134A. This produced the required one square wave per revolution signal necessary to trigger the Bently Nevada Digital Vector Filter. The digital vector filter produces DC outputs proportional to speed, amplitude and phase.

In Figure 5, the unfiltered amplitude of the hydrogen pump shaft motion is plotted against running speed during run-up to rated power level (RPL) for Run 902-065-7134. Considerable noise was found on this plot due to the high frequency components.

From the observation of the unfiltered signal, it is difficult to determine the location of the hydrogen pump critical speeds. Figure 6 contains only the synchronous component of the vibration in Figure 5, shows both run-up and run-down. These two plots illustrate the effect and the utility of using the synchronous tracking filter in unmasking the information contained in the vibration signals. Figure 6 shows peaks during run-up at 16,500 and 32,000 RPM which represents the first and second critical speeds. One should note that these peaks are not seen during run-down due to the rapid decelleration rate. At 28,000 RPM, the speed was held constant on run-up and a considerable reduction in vibration amplitude occurred. This phenomenon also occurred at rated power level (RPL). This drop in amplitude with time at constant rotational speed could be due to thermal changes in the system.

From Figure 6, an estimate of the bearing loading may be made. The shaft run-out is approximately 4 mils, while the peak amplitude at 32,000 RPM is 6.8 mils. Therefore, the relative motion at the second critical speed is approximately 2.8 mils. Assuming an effective stiffness of the bearing support system of 700,000 lb/in, a peak-to-peak load of 1,960 lbs is indicated. This is considerably in excess of the design radial bearing dynamic loading of 400 lbs. Since ball bearing life is inversely proportional to the bearing load cubed, the life of the bearings could be reduced by a factor of over 100 from the design value. For example, sustained operation under these conditions could cause a reduction of bearing life from 50 hrs to only 30 minutes.

In later runs, the proximity probe to investigate the shaft motion was not available due to bearing changes placed in the hydrogen pump. Therefore, accelerometer measurements had to be resorted to for the determination of the system resonance frequencies. The Spectral Dynamics SD360 digital signal processor and the Hewlett Packard 5420A digital signal analyzer, in conjunction with the Hewlett Packard 9845B computer and HP-9872A digital plotter, were used to evaluate some of the spectral characteristics of both hydrogen and oxygen pumps. For example, Figure 7 represents the time history wave form of the zero degree radial accelerometer for the hydrogen pump operating at 100% rated power level. The amplitude of motion of this signal is approximately $\pm$ 30 g's. On Figure 7 is shown one cycle of running speed. It is apparent that there are very high frequency components in the accelerometer signal. These high frequency components mask the structural modes of the rotor and casing near the operating speed. Figure 8 represents the same signal with low pass filtering applied. By filtering out the

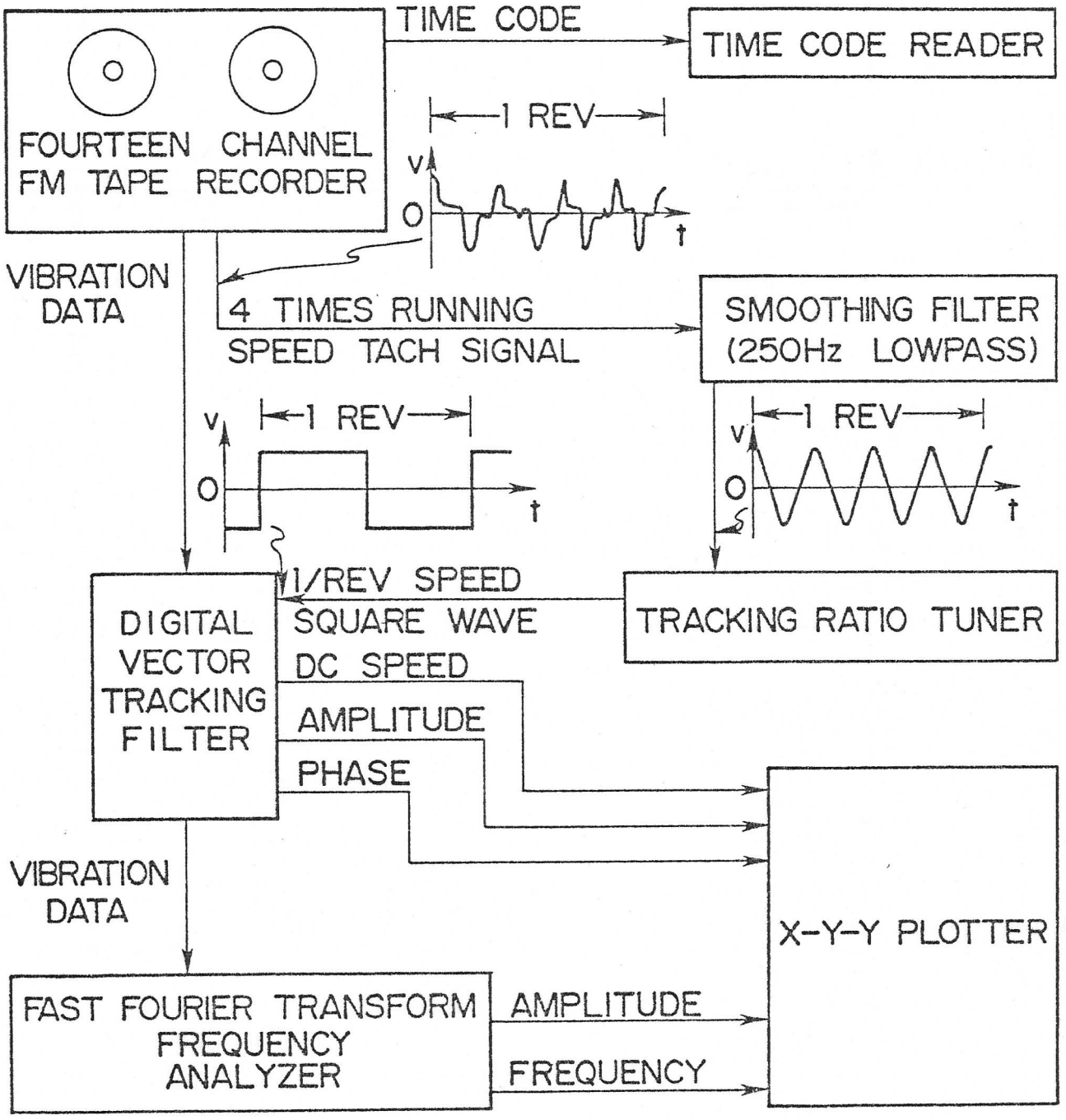

FIG 4 INSTRUMENTATION USED IN DATA REDUCTION

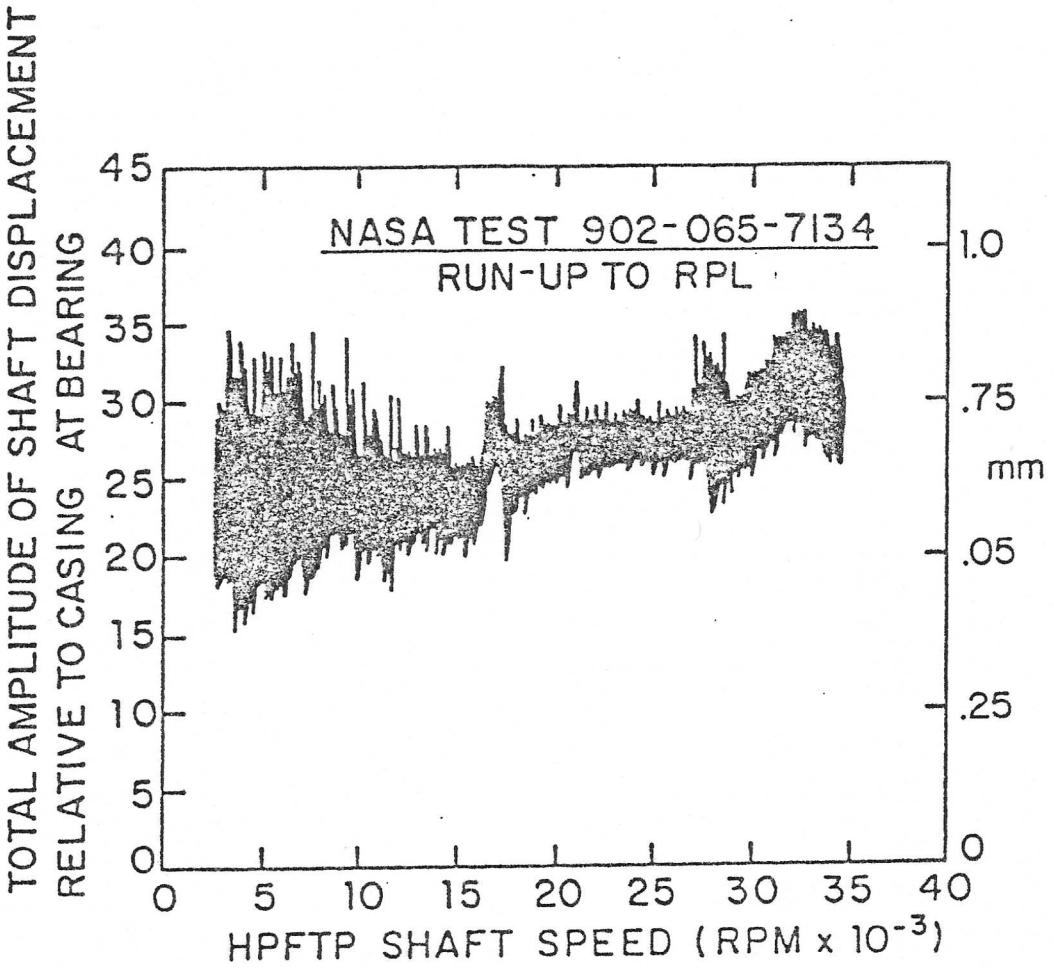

FIG 5 TOTAL HPFP SHAFT MOTION VERSUS HPFTP SPEED

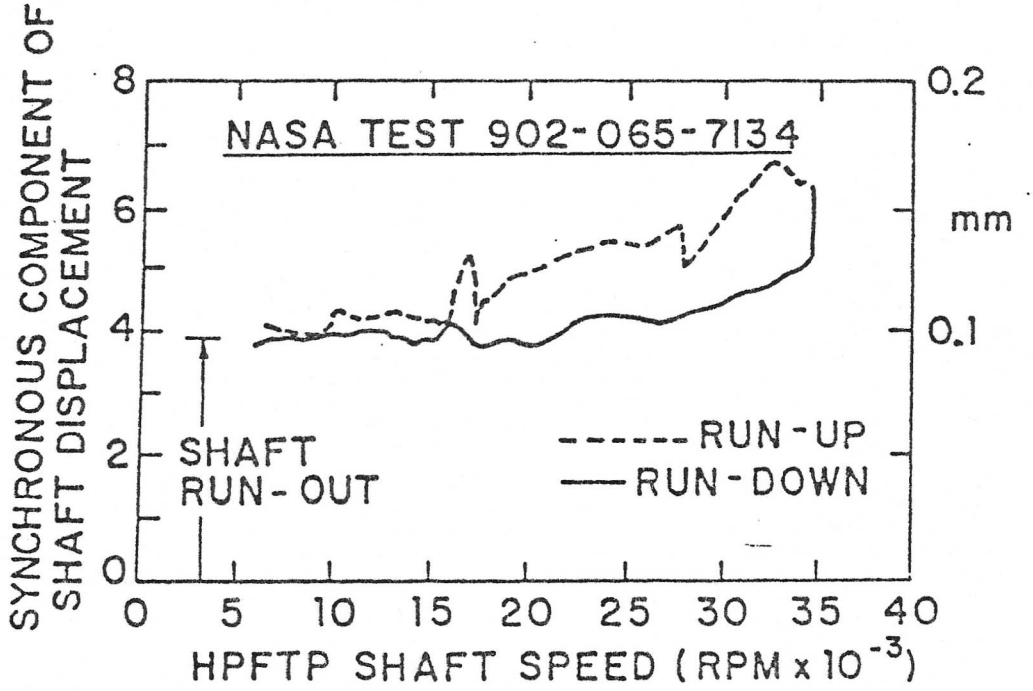

FIG 6 HPFTP SYNCHRONOUS MOTION

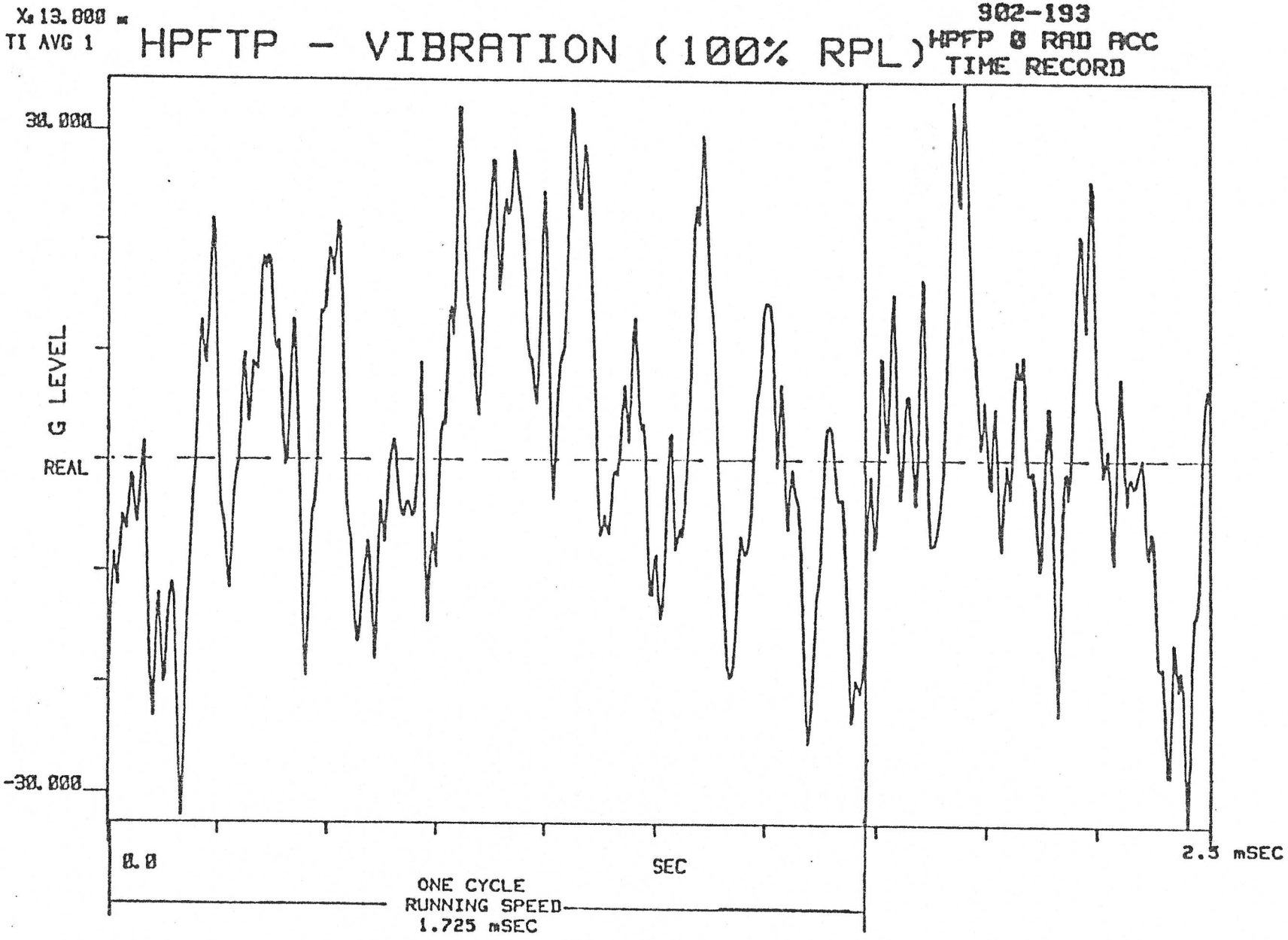

FIG 7 UNFILTERED WAVEFORM OF HPFP 0° RADIAL ACCEL. AT 100% RPL

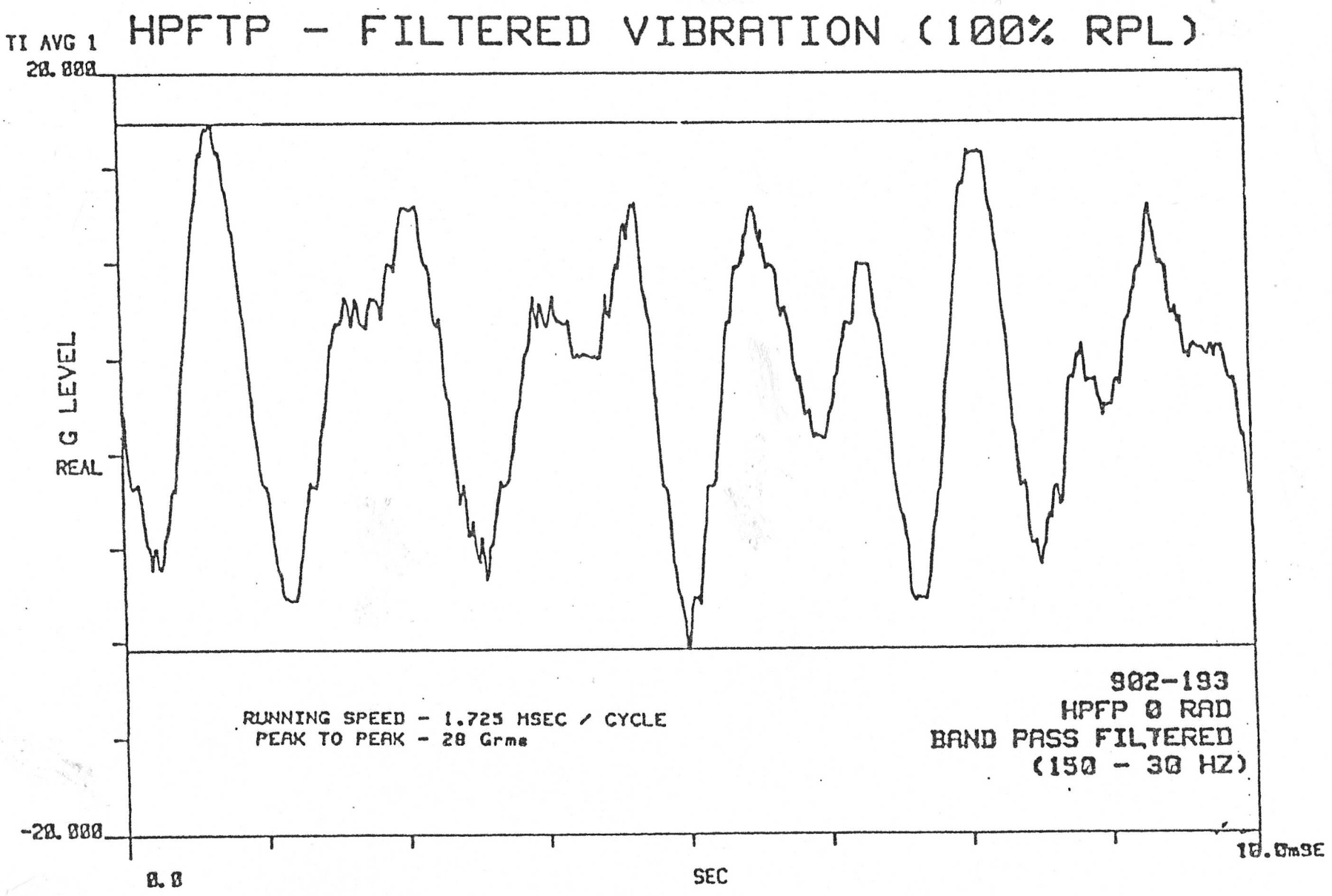

FIG 8 FILTERED WAVEFORM OF HPFP 0° RADIAL ACCEL. AT 100% RPL

higher frequency components that are several orders of magnitude above running speed, the frequency spectrum near the operating speed can be examined.

Figure 9 represents the peak channel-hold for the HPFT 90° accelerometer, with the higher frequencies filtered from the signal. By using the peak channel-hold procedure, one is able to capture the maximum spectrum produced by the pump. In this particular run, the engine was coasted down from 109% RPL to zero speed. It is apparent from the plot that there is a resonance frequency in the system at 591 Hz (35,460 RPM) which corresponds to the design operating speed of the hydrogen pump.

OXYGEN TURBOPUMP THEORETICAL ANALYSIS

The oxygen pump, labeled HPOTP, as shown in Figure 1 for high perssure oxygen turbopump, appears on one side of the figure. On the opposite side of the figure is the high pressure fuel turbopump, which supplies liquid hydrogen to the rocket nozzle. The liquid oxygen and hydrogen, supplied to the nozzles, are fed into the combustion chamber of the rocket engine. There are three rocket engines on each shuttle craft. The high pressure oxygen turbopump is designed to supply LOX (liquid oxygen) at 1,153 lbs per second to the engine. The supply pressure to the main pump is 4,974 psi and the supply pressure to the small preburner pump is 8,070 psi.

Figure 10 represents the cross-section of the HPOTP rotor. The rotor is supported at the pump-end (left) by two 45 mm ball bearings and at the turbine-end (right) by two 55 mm ball bearings. At the right, is shown the two-stage, hot gas turbine which drives the oxygen pump. The main pump is represented by the central impeller and is of a dual flow configuration.

The oxygen pump was designed to operate from 22,000 RPM (MPL--minimum power level) to 29,000 RPM (FPL--full power level) and is to be free of critical speeds in this vicinity. The design time of operation of the oxygen pump during FPL is 730 seconds.

Figure 11 represents the experimental data obtained during NASA test run 902-065. This figure shows the synchronous motion of a radial accelerometer as a function of oxygen pump shaft speed for both run-up and run-down. On run-up, two major resonant peaks are clearly seen: approximately 22,000 RPM and 27,000 RPM. Upon run-down, a very predominate peak at 26,000 RPM is observed. According to the original design specifications, there should not be any critical speeds in the operating speed range. However, later tests of the oxygen pump run in a balancing facility showed two critical speeds in the operating speed range. The 45 mm preburner bearing stiffness may be only of the order to 400,000 lb/in. Figure 12 shows the predicted oxygen pump mode shape with the reduced preburner bearing stiffness. The second critical speed is predicted to be 25,350 RPM (423 Hz).

OXYGEN TURBOPUMP EXPERIMENTAL INVESTIGATION

Proceedings similar to those used in the investigation of the hydrogen pump were used also on the oxygen pump with a few additional features. It was observed that hydrogen pump speed was often observed on the accelerometers on the oxygen pump casing. Therefore, it seemed desirable to investigate the influence of hydrogen excitation on the oxygen pump.

In order to evaluate the influence of the hydrogen vibration on the oxygen pump, an accurate hydrogen pump speed signal had to be superimposed on the oxygen vibration data. This was accomplished by dubbing in the hydrogen pump speed on the tape and synchronizing the recording by the use of two time code readers. By this means, it was possible to track the oxygen pump vibration as a function of hydrogen pump speed.

Figure 13 represents the same NASA test run (902-065) as in Figure 11, but in this case the synchronous motion of the oxygen pump casing accelerometer was tracked as a function of hydrogen shaft speed. Since the hydrogen pump operates at a slightly higher speed, the hydrogen pump acts as a vibration excitor, and the synchronous tracking filter (synchronous with the hydrogen pump speed) produces an indication of which resonant frequencies are within this operating speed range.

From the curve on run-up, it is seen that there is a resonant frequency at approximately 25,000 RPM. This information corresponds with the vibration data obtained on run-up and run-down as a function of hydrogen or oxygen pump speed. Also observed is a resonant frequency at approximately 28,000 RPM. Upon run-down, this is the predominate frequency observed. From this data, it therefore appears that there are three distinct resonant frequencies in the operating speed range. These resonant frequencies are approximately 22,000 RPM, 26,000 RPM, and 28,000 RPM. A 540° phase shift was observed which indicates the passage through three resonant frequencies (4).

Figure 14 represents the frequency spectrum obtained on NASA run 902-119 for the preburner axial 90° accelerometer for speeds ranging from 60° RPL to 100% RPL. In this figure, one is able to discern a low level oxygen pump motion which may be associated with the whirl of the oxygen pump at the first critical speed. This

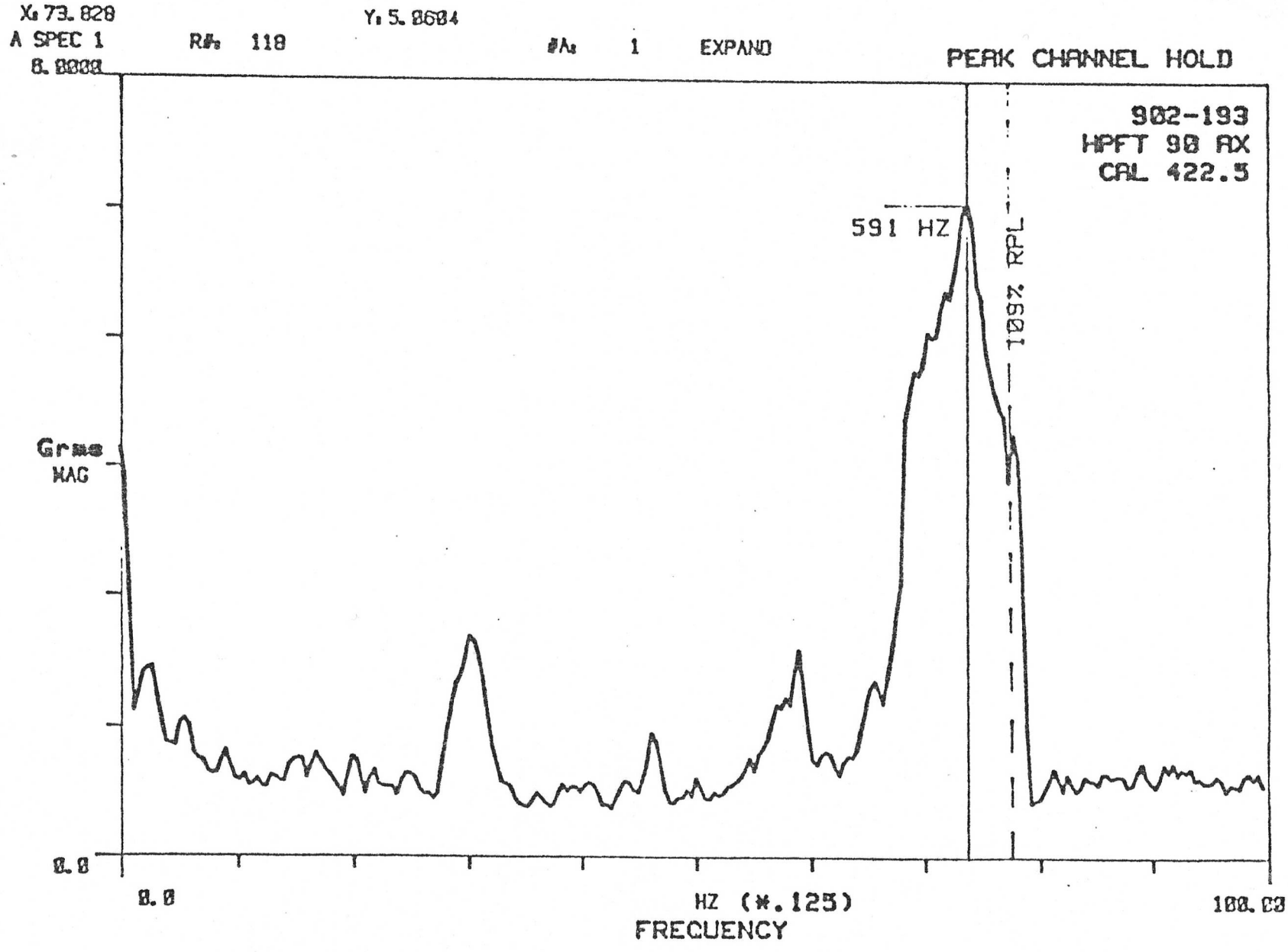

FIG 9 PEAK CHANNEL HOLD OF HPFP 90° AXIAL ACCELEROMETER FROM 109% TO 0% RPL

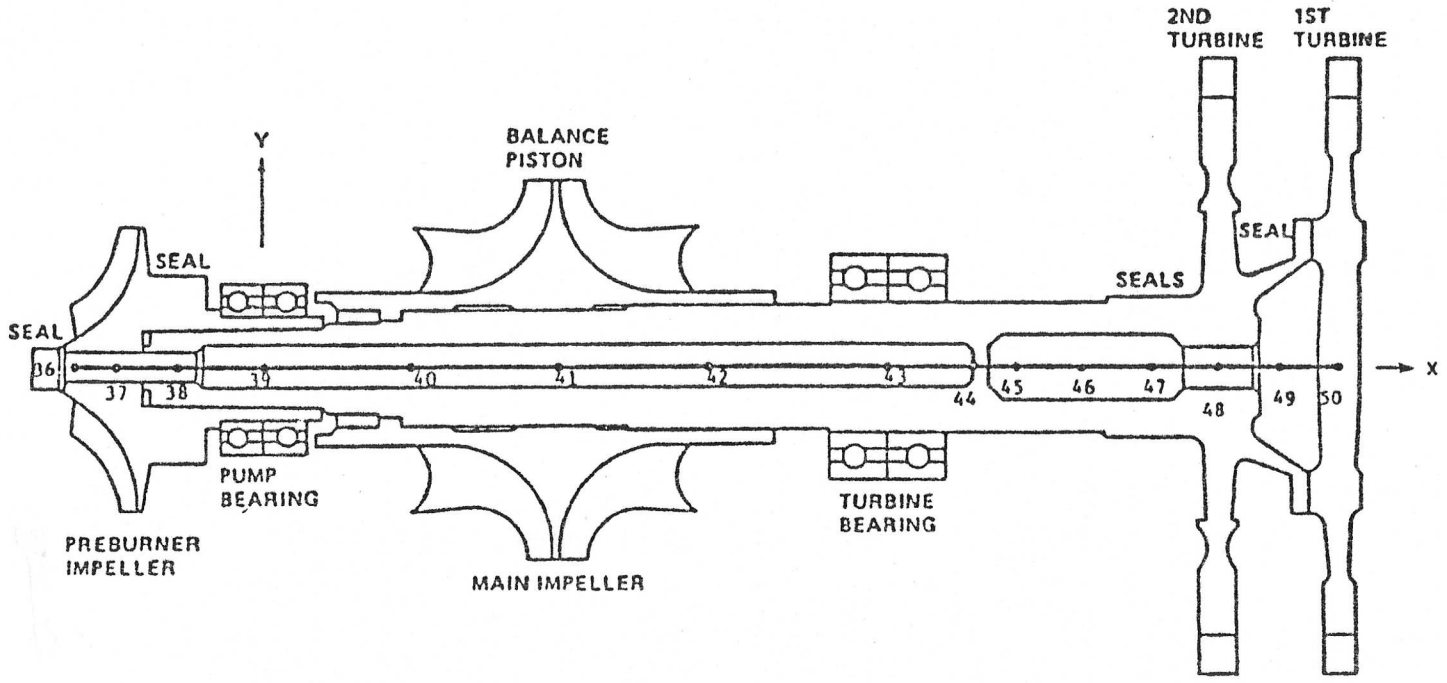

FIG 10 OXYGEN PUMP

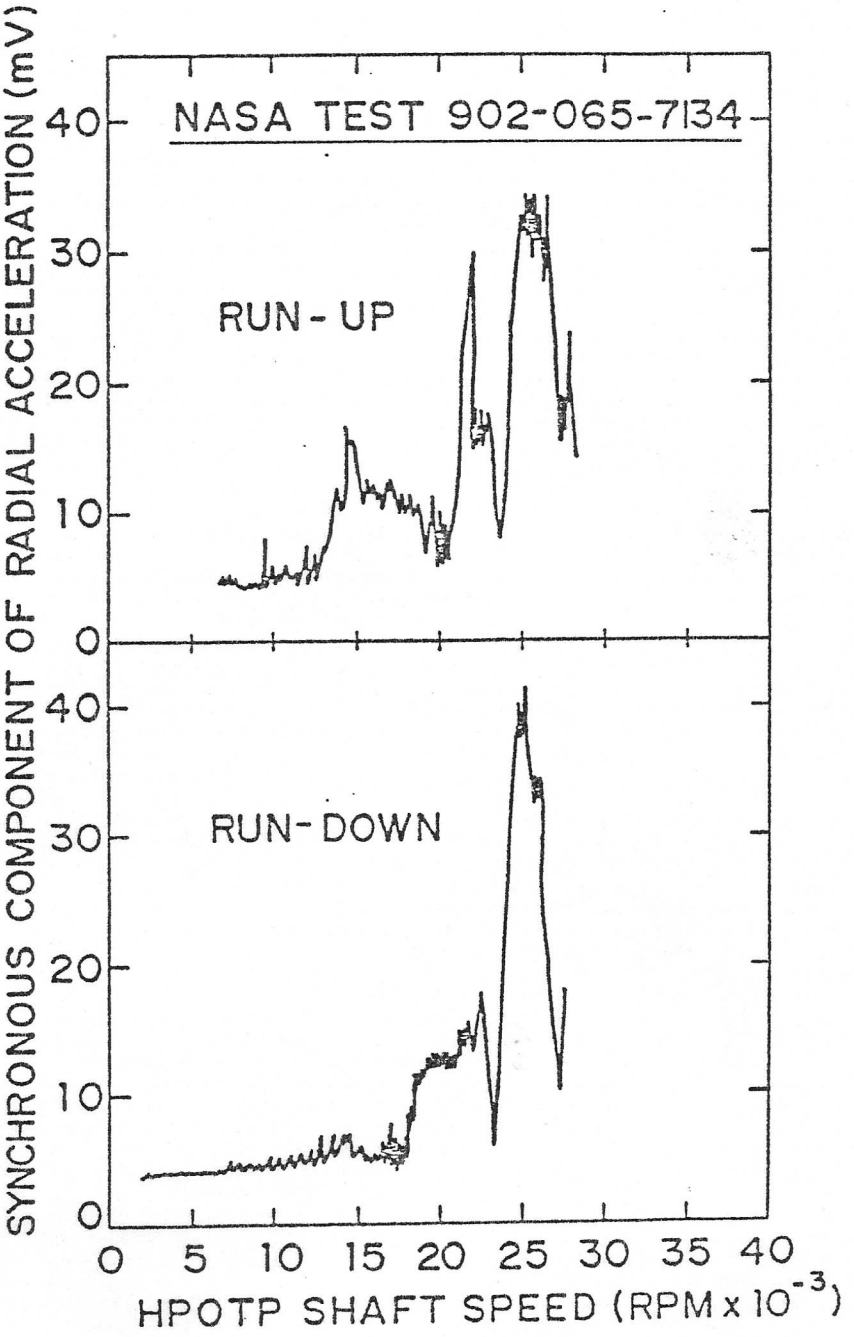

FIG 11 SYNCHRONOUS HPOT RADIAL ACCELEROMETER OUTPUT

VERSUS

HPOTP SPEED

N_{2f} = 25,350 RPM

K_p = 400,000 LB/IN

K_t = 600,000 LB/IN

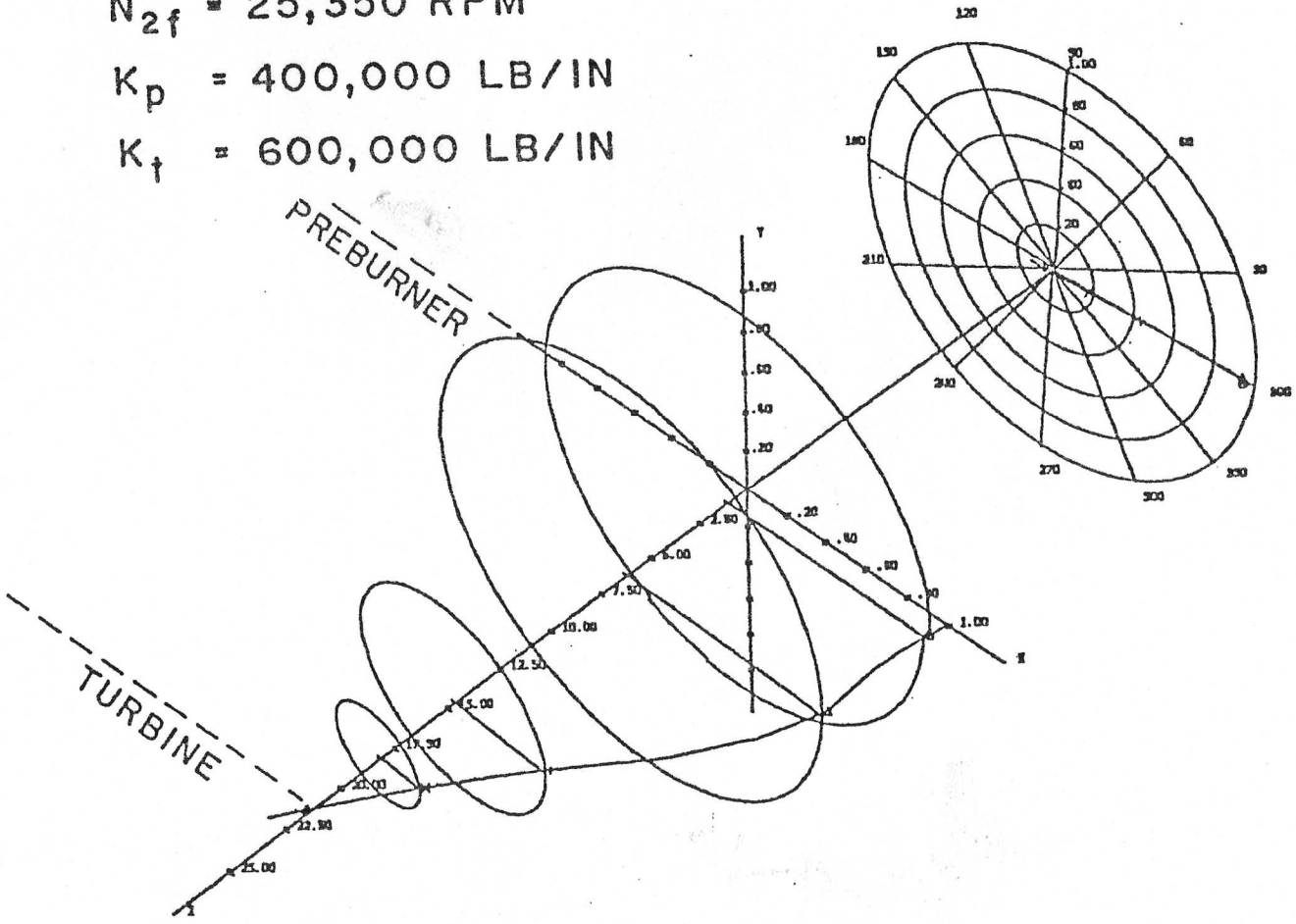

FIG 12.

UNDAMPED 2ND FORWARD CRITICAL SPEED OF

OXYGEN PUMP AT 27,000 RPM

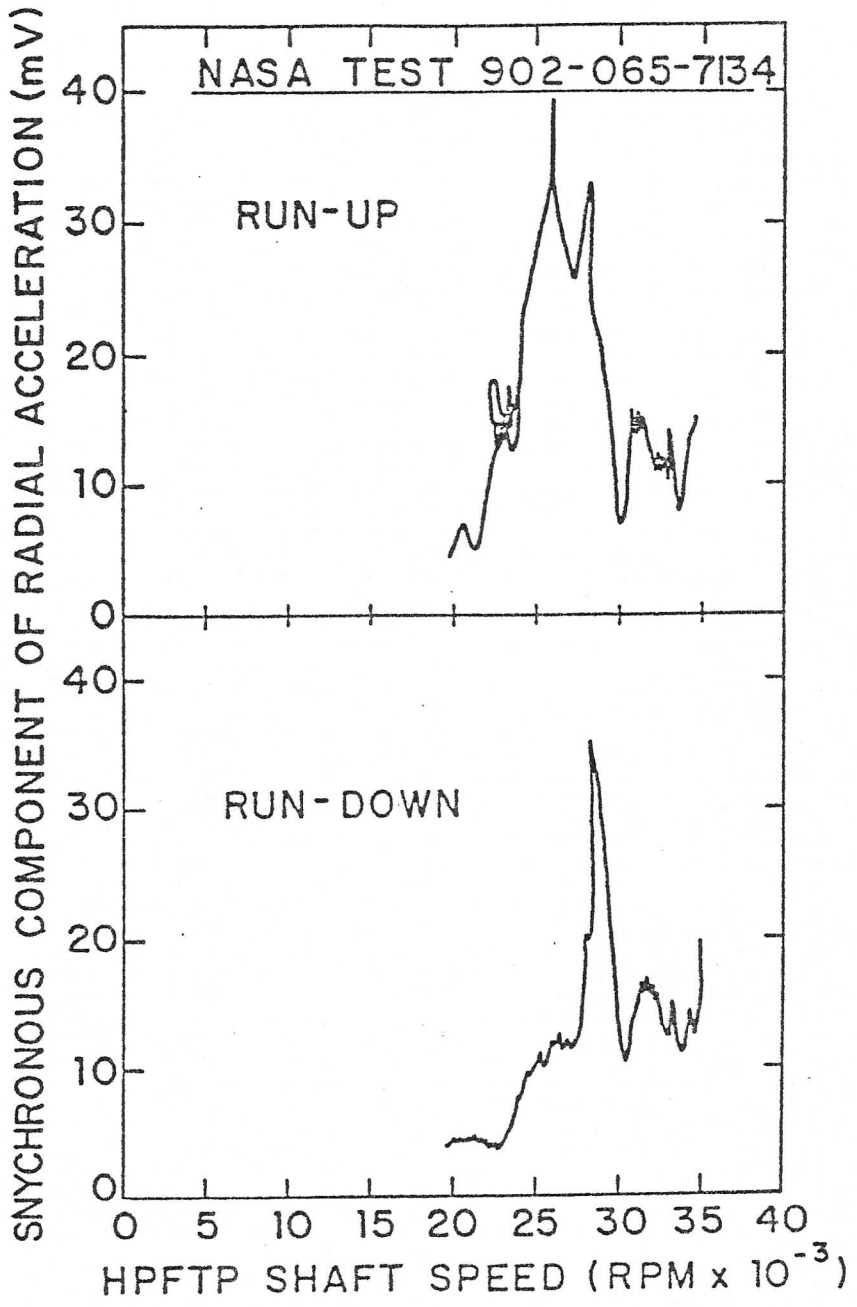

FIG 13 HPOT RADIAL 45° ACCELEROMETER VIBRATON AS A FUNCTION OF PUMP SPEED

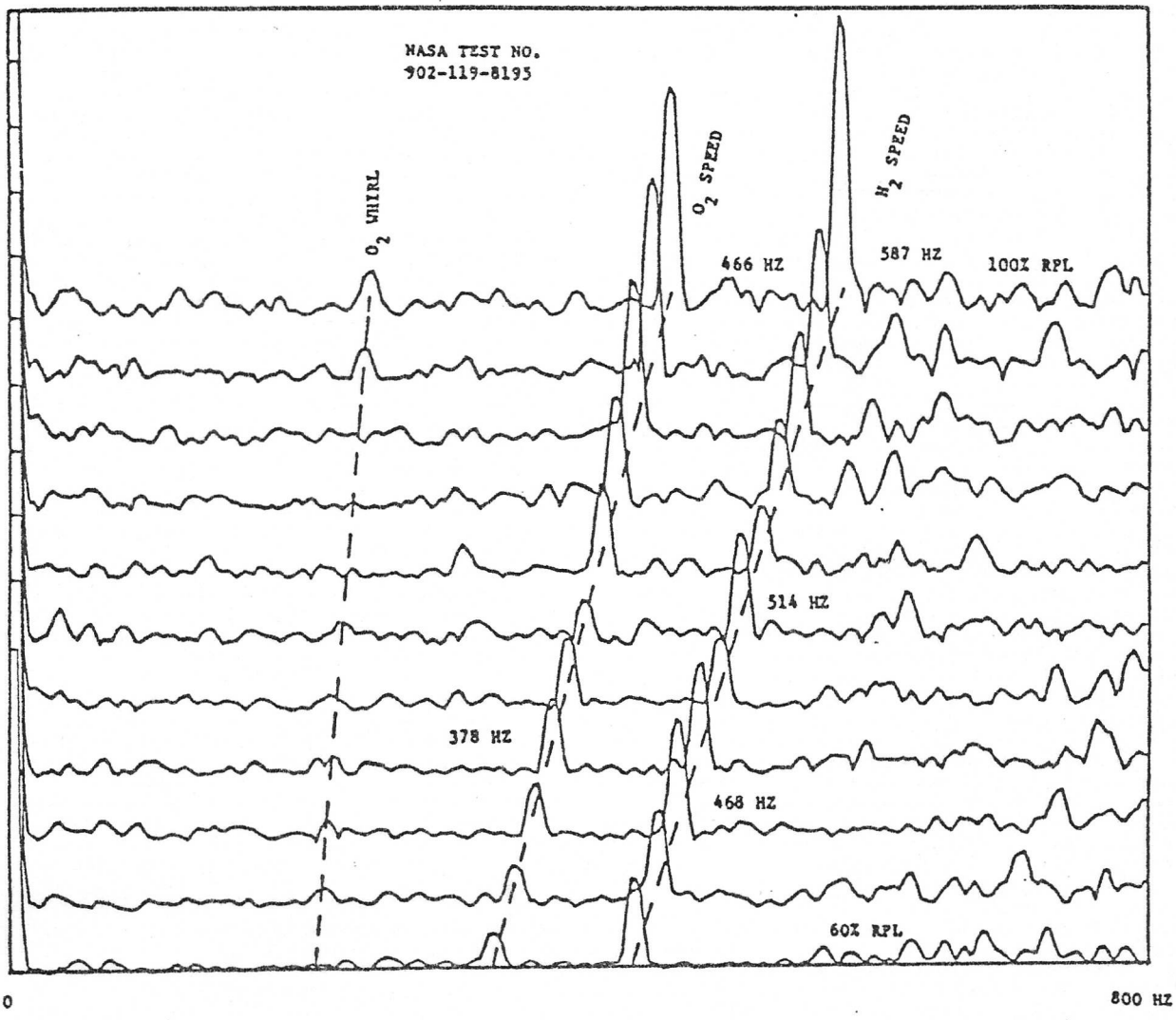

FIG 14

HPOP AXIAL 90° ACCEL.

CASCADE DIAGRAM

dotted line is designated "O_2 whirl". The frequency spectrum also shows the amplitude due to oxygen pump speed and to hydrogen pump speed. The frequency spectrum shows that there is an oxygen pump resonant frequency at approximately 378 Hz and at 466 Hz (which corresponds to 100% RPL). The amplitude increase indicates a possible resonant speed. The hydrogen pump speed is also clearly seen on this figure with peaks at 468 Hz, 514 Hz, and at 587 Hz (the operating speed of the hydrogen pump). It appears that the hydrogen pump may also be operating on a resonant frequency. The fact that the hydrogen pump speed peaks at 468 Hz also indicates a possible oxygen pump resonant frequency at the hydrogen pump operating speed.

During the course of the experimental testing of the SSME, there were several incidences in which malfunction of the oxygen pump occurred. One of these earlier incidences was Run 901-136-7251. Figure 15 represents the data recorded for this run. The engine was programmed to operate at 90% RPL for 31 sec, then increase speed to RPL and then return to 90% of rated power level for the rest of the run.

From the examination of this raw data (which was band passed from 250 to 500 Hz) it was seen that when the incident occurred the amplitudes were increasing rapidly on the preburner (PB) pump radial and HPOP axial accelerometers. The HPOT radial accelerometer output after 180 seconds actually decreased in value while the PB pump radial 45°, 135°, and HPOP axial accelerometer outputs increased rapidly. It therefore appears that at the time of failure, the casing had a considerable cantilever mode of motion in which there was both radial and axial displacement. This type of data does not, however, give much insight as to the speeds at which critical speeds or various resonant modes are occuring.

Figure 16 represents the synchronous radial acceleration of the oxygen rotor as a function of oxygen pump shaft speed (NASA test 910-136) using the synchronous tracking facilities of the Rotor Dynamics Laboratory of the University of Virginia.

During run-up, two resonances were observed at 22,000 and 25,500 RPM. The resonance at 25,500 RPM appears to dominate. This speed corresponds to operation at 90% rated power level. Upon reaching rated power level, the speed was reduced and the rotor was operated at 90% RPL. Due to continued operation at this speed, the rotor amplitude increased until failure occurred. The upper figure represents the phase angle change while passing through the 25,000 RPM speed range. The 180° phase shift shown corresponds to passage through a resonant frequency.

Figure 17 represents the peak channel hold accelerometer spectrum of the HPOP 45° radial accelerometer during deceleration from 109% to 90% RPL. Note that there is a pronounced resonant frequency at 463 Hz. The magnitude of the peak amplitude is 10 gms. Examination of the various other accelerometers on the oxygen pump showed a similar characteristic.

The data of Run 902-193 indicates that the oxygen pump has a major resonant frequency between 450 and 470 Hz. This response frequency could represent the second critical speed of the oxygen pump. This mode may be particularly sensitive to excitation, because a nozzle bending mode is also predicted in this range.

SUMMARY AND CONCLUSIONS

The high pressure hydrogen and oxygen pumps were instrumented with accelerometers and other instrumentation after excessive vibrations were observed on the SSME. This paper presents various procedures by which the vibration data was analyzed. Two basic types of instrumentation were used by the Rotor Dynamics Laboratory of the University of Virginia in the data reduction: synchronous tracking filters and fast Fourier signal analyzers. The synchronous tracking filters were used to observe pump and casing resonance frequencies as a function of hydrogen and oxygen pump speed. This procedure facilitates the identification of pump, or structural resonance frequencies in the operating speed range. The synchronous tracking procedure requires a properly conditioned pump speed reference signal. However, an adequate speed signal was not always available for use in certain NASA test runs of the SSME.

In this study, by the Rotor Dynamics Laboratory, the FFT analyzers were used exclusively for those cases where synchronous tracking could not be performed. FFT analysis was used to observe frequencies over various band widths. By using the FFT analyzer, one is able to generate a frequency cascade plot of the vibration spectrum for various engine power levels. This procedure, for example, showed that various frequencies may be observed from an accelerometer.

Overall, by using these types of instrumentation, one can obtain an understanding of the resonant frequencies and mode shapes of a vibrating structure. By correctly interpreting such data, one can recommend corrective measures by which the vibrations can be reduced.

ACKNOWLEDGEMENTS

The authors would like to acknowledge the assistance of Lyle A. Branagan,

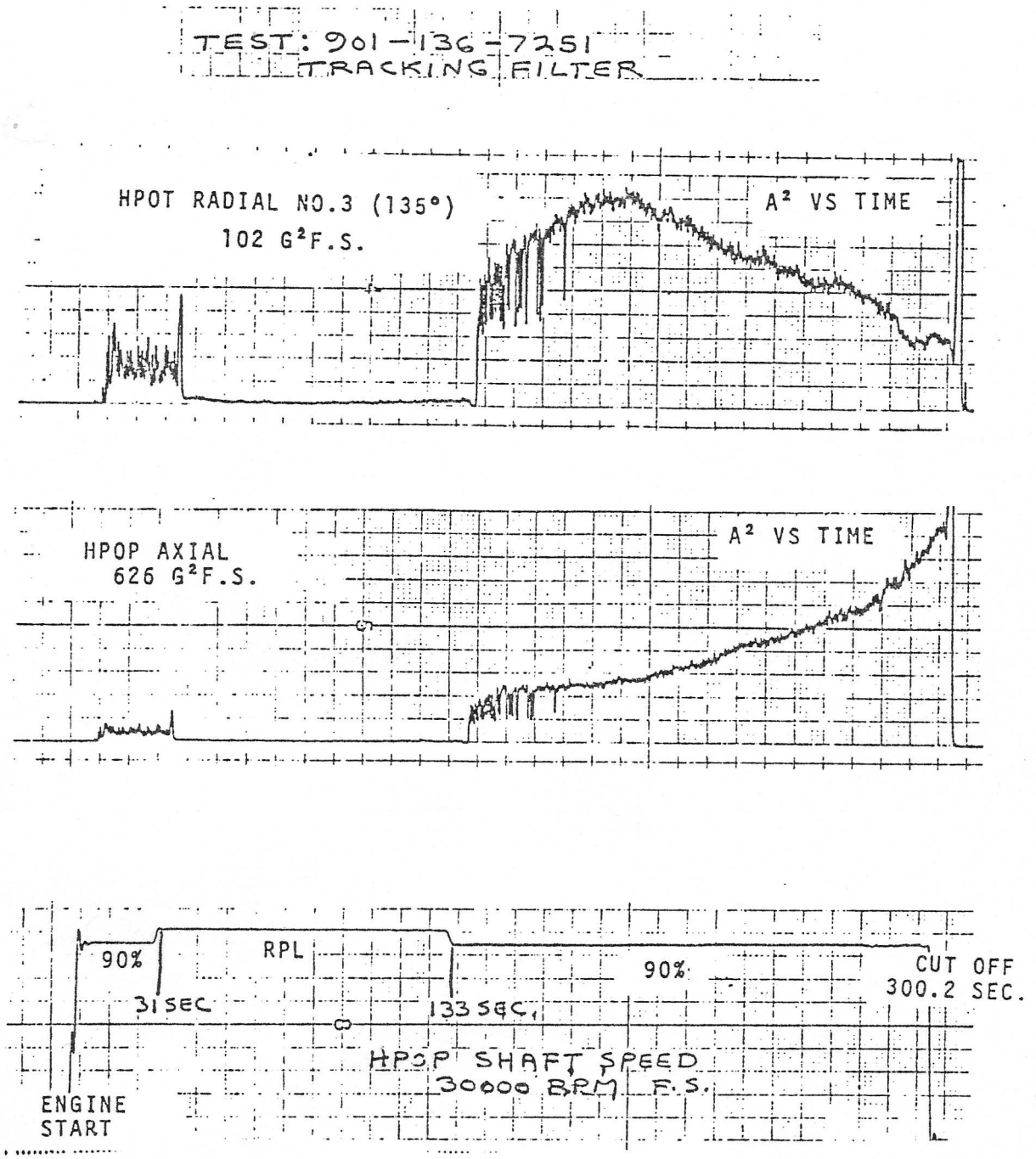

FIG 15 HPOP SYNCHRONOUS MOTION FOR HPOP

RADIAL ACCEL. DURING FAILURE RUN

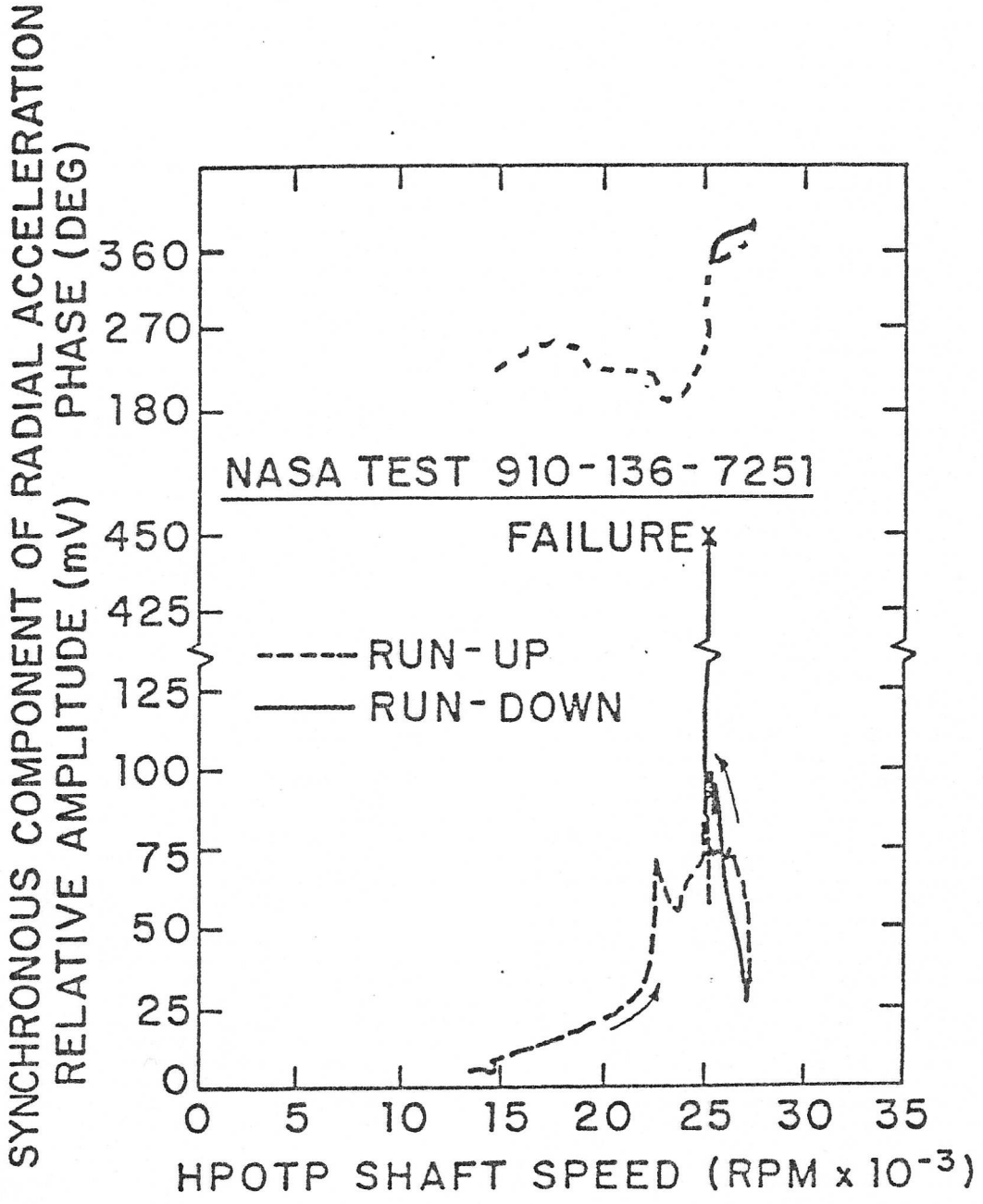

FIG 16 SYNCHRONOUS HPOT NO. 3 RADIAL ACCEL. VERSUS SPEED

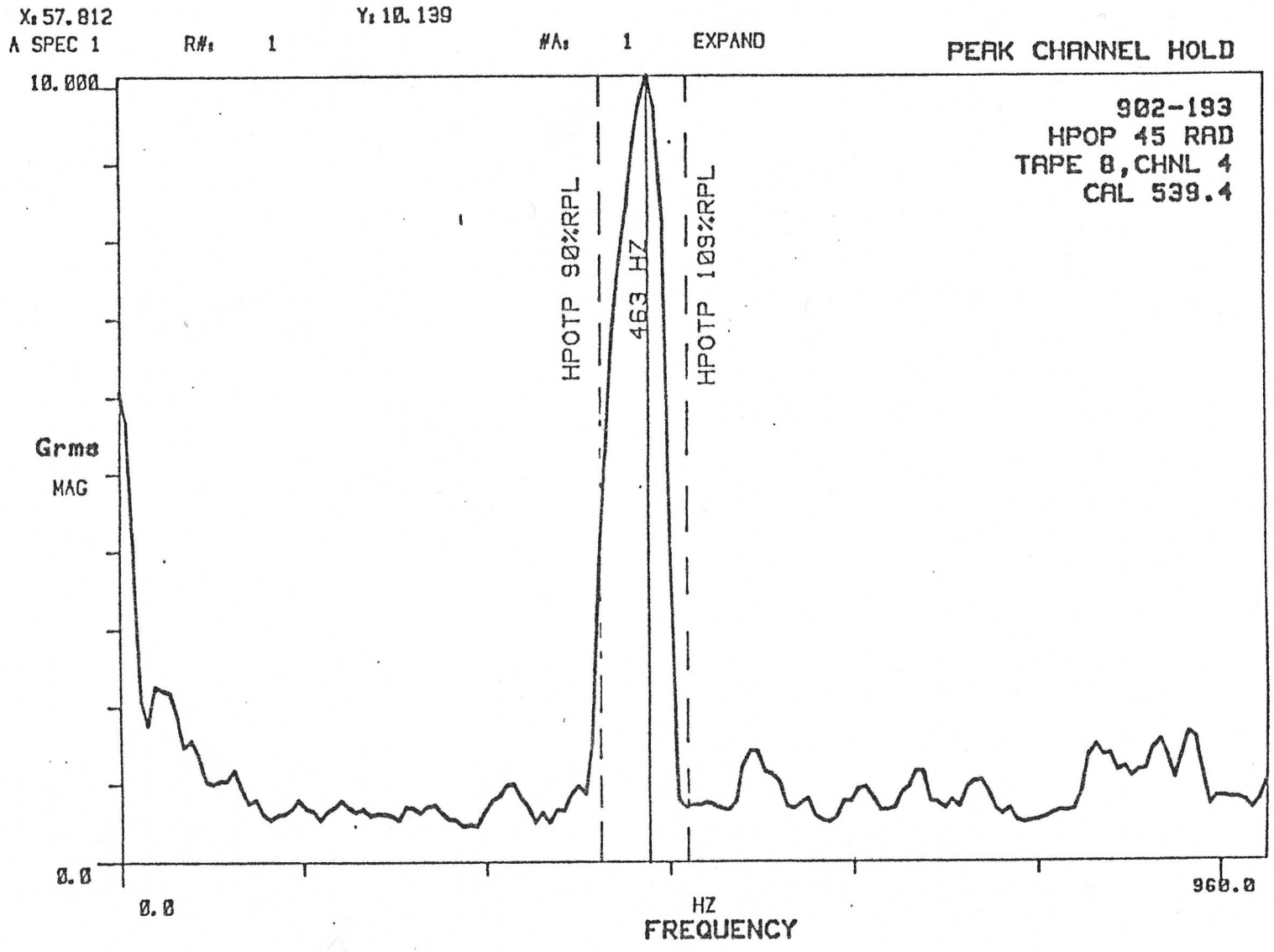

FIG 17

HPOP 45° RADIAL ENGINE DECELLERATION (109-90% RPL)

John D. Heinzmann and Alan B. Palazzolo, who helped with the data reduction. This work was supported by NASA Marshall Space Flight Center under Contract NAS8-31951-15. The authors particularly wish to express their appreciation to project monitors Otto Goetz and William D. Clarke for their encouragement and support on this project.

REFERENCES

(1) Childs, D. W., "The SSME High Pressure Fuel Turbopump Rotordynamic Instability Problem", Transactions of the ASME Journal of Engineering for Power, Paper No. 77-GT-49, December 1976.

(2) Allaire, P. E., Gunter, E. J., Lee, C. P. and Barrett, L. E. "Final Report - The Dynamic Analysis of the Space Shuttle Main Engine - High Pressure Fuel Turbopump, Part II - Load Capacity and Hybrid Coefficients for Turbulent Interstage Seal", Report No. UVA/528140/ME76/103, University of Virginia, Charlottesville, Va., September 1976.

(3) Gunter, E. J., Barrett, L. E., Palazzolo, A. B. and Allaire, P. E. "Final Report - The Dynamic Analysis of the Space Shuttle Main Engine - High Pressure Fuel Turbopump, Part III - Linearized Stability Analysis", Report No. UVA/528140/ME76/104, University of Virginia, Charlottesville, Va., September 1976.

(4) Eck, M. C. "Solution of the Subsynchronous Whirl Problem in the High Pressure Hydrogen Turbomachinery", Paper No. 78-1002, American Institute of Aeronautics and Astronautics 14th Joint Propulsion Conference, Las Vegas, Nev., July 25-27, 1978.

(5) Gunter, E. J., Li, D. F., Allaire, P. E. and Barrett, L. E. "The Dynamic Analysis of the Space Shuttle Main Engine - High Pressure Fuel Turbopump, Part I - Critical Speed Analysis", Report No. UVA/528140/ME76/102, University of Virginia, Charlottesville, Va., September 1976.